IEEE Access
Multidisciplinary | Rapid Review | Open Access Journal

Received August 7, 2021, accepted August 25, 2021, date of publication September 3, 2021, date of current version September 17, 2021.

Digital Object Identifier 10.1109/ACCESS.2021.3110477

An Improved Direct Torque Control Topology of a Double Stator Machine Using the Fuzzy Logic Controller

FLAH AYMEN[1], NAOUI MOHAMED[1], SAAD CHAYMA[1], C. H. RAMI REDDY[2], (Member, IEEE), MOSLEH M. ALHARTHI[3], AND SHERIF S. M. GHONEIM[3], (Senior Member, IEEE)

[1]Processes, Energy, Environment and Electrical Systems, National Engineering School of Gabès, University of Gabès, Gabes 6052, Tunisia
[2]Department of Electrical and Electronics Engineering, Malla Reddy Engineering College (Autonomous), Secunderabad, Telangana 500100, India
[3]Electrical Engineering Department, College of Engineering, Taif University, Taif 21944, Saudi Arabia

Corresponding author: Flah Aymen (flahaymening@yahoo.fr)

This work was supported by Taif University Researchers Supporting Project, Taif University, Taif, Saudi Arabia, under Grant TURSP-2020/122.

ABSTRACT In this paper, a dual stator induction machine is studied. This nonlinear system is built on the Matlab/Simulink tool to test the efficiency of the direct torque control loop for controlling this complicated system. It makes the speed and torque tracking more comfortable. On the other side, it is mandatory to assure the independence of the electrical alimentation of the dual stator. All these goals are guaranteed with this direct torque control technique. The conventional direct torque control loop is based on the switches' controllers. This method makes many fluctuations in the speed performances, the flux evolution, and the electromagnet torque progress. The conventional direct torque control drawbacks are resolved by improving this control loop using the fuzzy control topology. Then, an improved direct torque control loop using the intelligent controllers is presented to control the torque and speed of a dual stator induction machine and supervise the two stator fluxes and currents. Matlab/Simulink tool was used for implanting this innovation and showing the behavior of the results.

INDEX TERMS Direct torque control (DTC), fuzzy logic controller, vector modulation, simulation, Matlab, performances, dual stator machine.

I. INTRODUCTION

Electrical motors were used mainly in blowers, pumps, fans, and machine tools applications. Until nowadays, this machine is essential in all production lines and manufacturers. Recently, it is integrated into the renewable energy field and electrical transportation tools. A variety of models exist, and the basic design was based on the continued current alimentation. Then, the new models appeared, and the alternating current machine was more suitable for such applications. Some special machine designs were presented to improve the efficiency of complicated applications, such as the renewable energy wind system or the electric vehicle transport system. These applications need a small motor and a high torque factor, and others require a high-power efficiency for low speeds. The permanent magnet machines were then designed, and the dual stator machine and the dual rotor motor were also exposed to resolve some of these problems. If concentrating on electric vehicle applications and efficiency, which needs a high-power machine with a small size, and if focused on low wind speed in some situations, the dual stator machine was resolved some of these problems.

The invention of double stator machines was appeared in the early 1900s [1]. Muñouz and Lipo [2] introduced it. The interest in this type of machine has increased for motor and generator-based applications because it offers certain advantages over conventional machines [2]. Those benefits are related to the possible extended operating range, including low-speed operation and full utilization of the stator windings [3]. But the coupling between the two stators, which produces circulating currents if the voltages are not perfectly balanced, is the only drawback of this machine. So, such

The associate editor coordinating the review of this manuscript and approving it for publication was Nishant Unnikrishnan.

control solutions were proposed to address this problem. These control loops were based on the pulse-width modulation systems, as explained in [4]–[6].

The dual stator induction machine consists of two three-phase stator windings, the stator ''1'' and the stator ''2'', and a common squirrel-cage rotor winding. The two stators can be shifted by one angle α, and they have two different pairs of poles. Usually, the stator poles are selected in a ratio of 1:3 (e.g., 2:6 or 4:12) [7]. Thanks to the use of two stators and power converters, reliability has been improved, making the stator configuration very suitable for applications where robustness has top priority, such as automotive [8] traction drives [9] propulsion and generation [8], [10].

In this type of machine, two inverters can control the motor, controlling two simple machines independently. This aspect is considered an exciting feature for such applications [10]–[12]. So, the conventional control methods applied for three-phase induction motors can also be applied to the Dual stator machine [13], [14], such as the Direct Torque Control (DTC) method [15], [16] and the field-oriented vector control loop [17]. The direct torque control was more robust and straightforward for these induction machines and directly controlled the torque. Contrary to field-oriented vector control, which needs a complicated mathematical analysis and a high processor calculator, variables conversations [18]. The DTC method uses an attractive approach because of its high efficiency and simplicity of implementation. This technique allows calculating control quantities (stator flux and electromagnetic torque) from the stator current measurements without a mechanical sensor [19], [20]. The basic weaknesses of this method are attributed to the online estimation of flux, electromagnet torque, and its primary version. The basic architecture of the Direct Torque Control, which uses hysteresis controllers, demonstrated many ripples and fluctuations on the different variable output, such as the magnet flux, currents, speed, and electromagnet torque. This phenomenon is principally related to the controller architecture and its parameters that need optimization [19]. Therefore, numerous methods and solutions were designed and implemented for resolving these problems. Based on the neural network technique and fuzzy logic controller, some of these solutions have better performances in the low-speed control regions and others have a better performance for high speeds. If concentrating on the neural network solution, Many problems were encountered in the learning steps, and this method requires big database information and a high-speed processor tool [21]. Even the database has more information and more cases about the system in its function mode, and the controller will be perfectly built and be more robust. The robustness of such neural controller, face some exterior or interior phenomenon will be assured even similar cases exist in the database for the learning step. The control machine field can't fix how much the needed database is extensive, even if it contains more cases and situations, even the overall system be stable and robust [22], [23]. This specification does not exist for the fuzzy logic controller. Even if the controller is not formatted correctly, it is easier to adjust its rules, which is not the case for the neural network controller, as this needs a new learning step for adjusting the used controller.

The fuzzy logic controller was also used for improving the DTC architecture, and the results prove that the performance becomes better. However, the known architecture and test were given and applied for the simple induction machine and is not guaranteed in the dual stator machine, as the coupling problem exists between the two stators. The rules discerption will be multiplied by two, and the conditions will be more complicated [22]. In [23], authors have applied the fuzzy controller, for controlling symmetrical the two stators and the rules are dependent. Here, a bloc of decoupling was used to avoid the previously cited problem. This method will complicate the interior control loop of the machine.

So, working on the dual stator machine presents the principal paper objective. The main point of this research is to give the corresponding direct torque control architecture adapted for this complicated machine design and resolve the ripples and fluctuations problems using the fuzzy logic solution. Furthermore, the proposed control pack assures the independence between the two stators alimentation and validation, which presents another key of this paper. This issue will resolve the problems confronted by authors in these references [25], [26] and related to the system's instability in other control solutions.

Matlab Simulink tool was used to design all the necessary blocs and visualize the different parameters and variables. Initially, an introduction section starts this paper. Then a general discerption of the utility of the dual stator machine in two applications as renewable energy and electric vehicle is discussed. The corresponding mathematical model is given in the third section and next, the direct torque control loop is designed and explained. The fuzzy DTC configuration was delivered and presented in the next section by citing the necessary fuzzifications and rules phases. In the fifth section, the results are provided and discussed. Finally, a conclusion part resumes the paper objectively and cites selected perspectives for this work.

II. APPLICATIONS USING DUAL STATOR MACHINE

Special electric machines appeared in this last decade, and a lot of versions were developed. Some Special machines are based on a double stator, others on a double rotor are based on a particular material inside their stator or rotor parts. Conventionally, the machines based on the magnet material have better performances. However, the high price of these machines makes them difficult to be primarily used. The dual stator machine presents numerous advantages for two recent renewable research fields, especially for electric vehicles and wind energy applications. The advantages of this machine and their weaknesses can be cited as follow. For an electric vehicle application, the principal advantages of this machine are attached to the high given power, even the small size of this

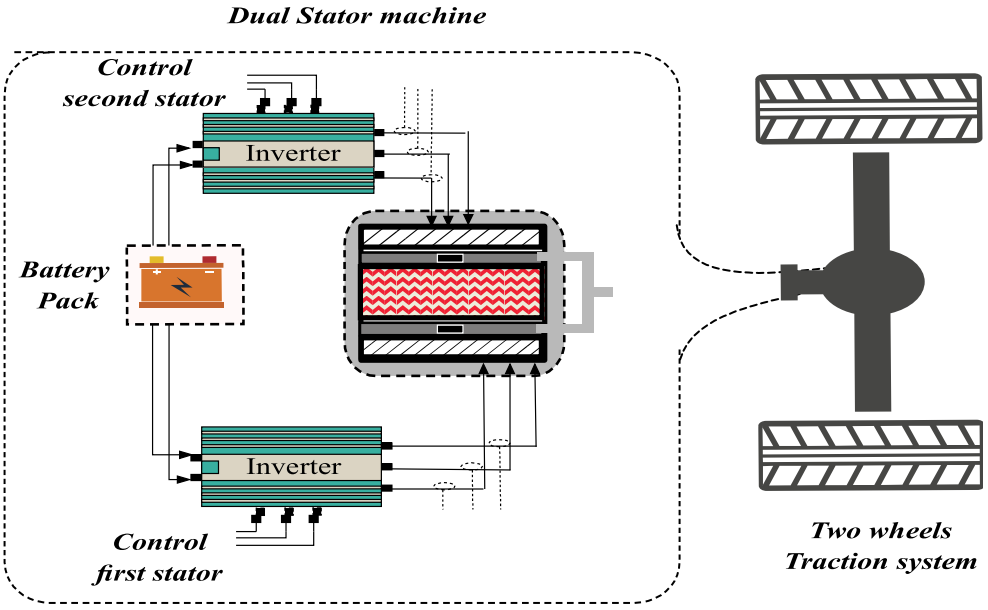

FIGURE 1. A dual stator machine used for electric vehicle application.

machine; however, a complex architecture is presented. Also, large noises will appear even the needed speed increases. In [17], the authors proved that it is possible to gain 1.5 L in the vehicle space when using this machine, contrary to the conventional permanent magnet machine, which is large. It will allow having increased vehicle autonomy and help to increase the vehicle speed and traction torque. This machine has numerous advantages for the other side and the wind energy field, but the most important factor is the large marge of speeds that allow large power. It makes the given power stable and eliminates any problem of rocking. Working on only one stator or dual stators is controlled according to the wind speed. For this case, the most important weaknesses can be supervised in the flux evolution, where two stators flux can be dependent, making the system unstable. Therefore, finding a robust control method is mandatory and will help increase each application's global efficiency.

A. APPLICATION FOR ELECTRIC VEHICLE FIELD

The dual stator machine (DSM) was found suitable for high torque application needs. It gives a possibility of increasing the electromagnet torque or the rotation speed when is needed. Such specification is recommended mainly in the traction application like the electric vehicle, scooter, based on two or only one wheel. A simple machine specifies a medium-sized machine in the same marge of power. In [17], authors proved that such machines' size and weight are smaller face other types. It increases the system autonomy and advances global efficiency, and will give more power and torque. In Fig. 1, the Dual Stator machine is coupled to the wheels system. For this application, the two stators will be connected to two independents three phases inverters. Only a battery pack is used to feed the machine with the necessary electrical power [24]. The control loop will be connected to each of the inverters separately. So, it is possible to control the two stators simultaneously or individually.

B. APPLICATION FOR THE RENEWABLE ENERGY FIELD

In the renewable energy field, wind energy is based on such electrical motors. Many types exist, and the dual stator machine is one of these motors. It is knower that wind speed is not constant. The adaptation of the electrical generator speed and the wind system speed must be controlled to secure the connection to the grid and protect all electronic equipment. The benefit of this special machine can be visualized when there are various wind speeds, especially in lower-speed cases. Actually, in this case, the provided power will be minimum, and then it is possible to integrate the other stator to increase the delivered power to the grid. It will allow having more power even the wind speed is low and then improve the efficiency of the wind system for all seasons. As shown in Fig. 2, a double stator is connected to the grid side through a rectifier and an inverter. The energy flow in the grid side was controlled in the first stator or the second stator. Also, the control of the two or only one stator is managed by a control algorithm, which selects the best situation face grid status and climatic situations.

III. MODELING OF THE DUAL STATOR MACHINE

As it is conventional, the control of a physical system must pass through the modeling phase to define all the inputs, variables, and parameters. In addition, it will allow defining the necessary signals that will control this machine. As dual three-phase stators exist and a coupled winding rotor is present, the corresponding mathematical models will be defined as follow:

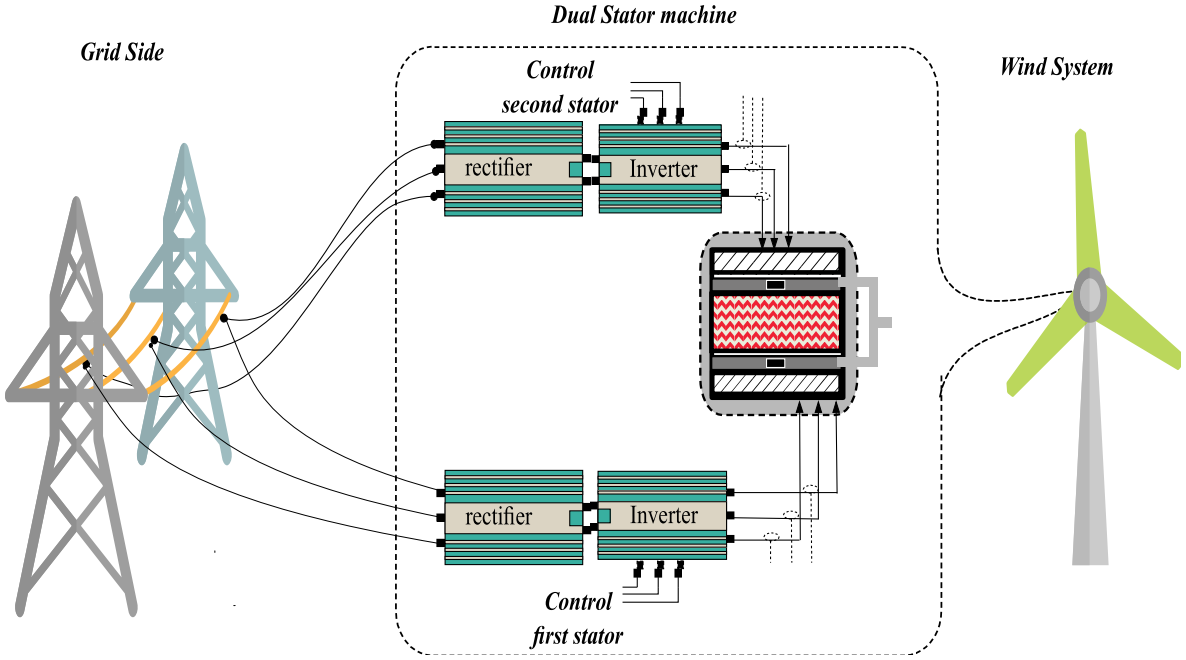

FIGURE 2. A dual stator machine used in the wind system.

A. ELECTRICAL EQUATIONS

Initially, it is required to cite the simplified hypotheses to facilitate some difficulties concerning machine behavior. Therefore, it is supposed that the air distance is uniformed, a low saturation factor, the stator winding distribution is sinusoidal, naturally insulated stator windings, and the current between bars is neglected [25]. The mathematical equations of the dual stator machine in a fixed reference to the stator can be written as follows:

The complex vector variable for the stator and rotor voltage and flux is given by equations (1) [26].

$$\begin{cases} \underline{v}_{s1} = r_{s1}\underline{i}_{s1} + p\underline{\phi}_{s1} \\ \underline{v}_{s2} = r_{s2}\underline{i}_{s2} + p\underline{\phi}_{s2} \\ r_r i_r + p\phi_r = 0 \end{cases} \tag{1}$$

The corresponding fluxes equations can be shown in equation (2).

$$\begin{cases} \underline{\phi}_{s1} = L_{s1}\underline{i}_{s1} + L_{s1r}\underline{i}_{r1} \\ \underline{\phi}_{s2} = L_{s2}\underline{i}_{s2} + L_{s2r}\underline{i}_{r2} \end{cases} \tag{2}$$

The proper stator inductance can be expressed as it is in equation (3). It is essential to indicate that i$\in$ [1, 2] and the adequate inductance of the rotor faces each of the two stators can be expressed as equation (4). a_n or x_n is the number of turns inside the rotor winding for the first or the second stator influence, respectively. The indices a, b and c are the voltage sources indices [27].

$$L_{si} = \begin{bmatrix} L_{lsi} + L_{msi} & -L_{msi}/2 & -L_{msi}/2 \\ -L_{msi}/2 & L_{lsi} + L_{msi} & L_{lsi} + L_{msi} \\ L_{lsi} + L_{msi} & -L_{msi}/2 & L_{lsi} + L_{msi} \end{bmatrix} \tag{3}$$

$$\begin{aligned} L_{s1r} &= \begin{bmatrix} L_{a1} & L_{a2} & \cdots & L_{a(n-1)} & L_{an} \\ L_{b1} & L_{b2} & \cdots & L_{b(n-1)} & L_{bn} \\ L_{c1} & L_{c2} & \cdots & L_{c(n-1)} & L_{cn} \end{bmatrix} \\ L_{s2r} &= \begin{bmatrix} L_{x1} & L_{x2} & \cdots & L_{x(n-1)} & L_{xn} \\ L_{y1} & L_{y2} & \cdots & L_{y(n-1)} & L_{yn} \\ L_{z1} & L_{z2} & \cdots & L_{z(n-1)} & L_{zn} \end{bmatrix} \end{aligned} \tag{4}$$

Also, the fluxes equations have been evaluated differently in another research. But, then, another mathematical presentation exists in the literature and uses the winding specifications as the angle between teeth and poles number and inductances values. So, equation (2) can also be written in this form of equation (5).

$$\begin{cases} \underline{\phi}_{s1} = \left(L_{sl1} + \dfrac{3}{2}L_{ms1}\right)\underline{i}_{s1} + \dfrac{n}{2}L_m e^{jp_1(\theta_r+\delta)}\underline{i}_{r1} \\ \underline{\phi}_{s2} = \left(L_{sl2} + \dfrac{3}{2}L_{ms2}\right)\underline{i}_{s2} + \dfrac{n}{2}L_m e^{jp_2(\theta_r+\delta)}\underline{i}_{r2} \end{cases} \tag{5}$$

It will allow a new presentation of the stator voltages equations, and equation (6) gives the new form.

$$\begin{cases} \underline{v}_{s1} = r_{s1}\underline{i}_{s1} + (L_{ls1} + \dfrac{3}{2}L_{ms1})p\underline{i}_{s1} + \dfrac{n}{2}L_{m1}e^{jp_1(\theta_r+\delta)} \\ \qquad\qquad (p + jp_1\omega_1)\underline{i}_{r1} \\ \underline{v}_{s2} = r_{s2}\underline{i}_{s2} + (L_{ls2} + \dfrac{3}{2}L_{ms2})p\underline{i}_{s2} + \dfrac{n}{2}L_{m2}e^{jp_2(\theta_r+\delta-\xi)} \\ \qquad\qquad (p + jp_2\omega_2)\underline{i}_{r2} \end{cases} \tag{6}$$

If concentrating on the rotor side, the expression of the fluxes vectors can be expressed as it is in equation (7), and then the rotor voltages expressions can be written as it is in

equation (8).

$$\begin{cases} \underline{\phi}_{r1} = L_{r1}i_{r1} + \frac{3}{2}L_{m1}e^{-jp_1(\theta_r+\delta)}\underline{i}_{s1} \\ \underline{\phi}_{r2} = L_{r2}i_{r2} + \frac{3}{2}L_{m2}e^{-jp_2(\theta_r+\delta-\xi)}\underline{i}_{s2} \end{cases} \tag{7}$$

$$\begin{cases} \underline{0} = r_{r1}\underline{i}_{r1} + L_{r1}\underline{i}_{r1} + \frac{3}{2}L_{m1}e^{-jp_1(\theta_r+\delta)}(p - jp_1\omega_r)\underline{i}_{s1} \\ \underline{0} = r_{r2}\underline{i}_{r2} + L_{r2}\underline{i}_{r2} + \frac{3}{2}L_{m2}e^{-jp_2(\theta_r+\delta-\xi)}(p - jp_2\omega_r)\underline{i}_{s2} \end{cases} \tag{8}$$

The mathematical description seems complicated, and the park/Clark transformation offers a better view to manipulate this nonlinear system. So, the new voltages equations can be summarized in equation (9), and the corresponding flux equations are summarized in equation (10) [28].

$$\begin{cases} \underline{v}_{qds1} = r_{s1}\underline{i}_{qds1} + jp_1\omega_1\underline{\phi}_{qds1} + p\underline{\phi}_{qds1} \\ \underline{v}_{qds2} = r_{s2}\underline{i}_{qds2} + jp_2\omega_2\underline{\phi}_{qds2} + p\underline{\phi}_{qds2} \\ \underline{0} = r_{r1}\underline{i}_{qdr1} + jp_1(\omega_1 - \omega_r)\underline{\phi}_{qdr1} + p\underline{\phi}_{qdr1} \\ \underline{0} = r_{r2}\underline{i}_{qdr2} + jp_2(\omega_2 - \omega_r)\underline{\phi}_{qdr2} + p\underline{\phi}_{qdr2} \end{cases} \tag{9}$$

where:

$$\begin{cases} \underline{\phi}_{qds1} = (L_{s1} - L_{m1})\underline{i}_{qds1} + L_{m1}(\underline{i}_{qds1} + \underline{i}_{qdr1}) = L_{s1}\underline{i}_{qds1} \\ \qquad\qquad + L_{m1}\underline{i}_{qdr1} \\ \underline{\phi}_{qds2} = (L_{s2} - L_{m2})\underline{i}_{qds2} + L_{m2}(\underline{i}_{qds2} + \underline{i}_{qdr2}) = L_{s2}\underline{i}_{qds2} \\ \qquad\qquad + L_{m2}\underline{i}_{qdr2} \\ \underline{\phi}_{qdr1} = (L_{r1} - L_{m1})\underline{i}_{qdr1} + L_{m1}(\underline{i}_{qdr1} + \underline{i}_{qds1}) = L_{r1}\underline{i}_{qdr1} \\ \qquad\qquad + L_{m1}\underline{i}_{qds1} \\ \underline{\phi}_{qdr2} = (L_{r2} - L_{m2})\underline{i}_{qdr2} + L_{m2}(\underline{i}_{qdr2} + \underline{i}_{qds2}) = L_{r2}\underline{i}_{qdr2} \\ \qquad\qquad + L_{m2}\underline{i}_{qds2} \end{cases} \tag{10}$$

With ω_1 and ω_2 is the electrical rotating speed and ω_r is the rotor electrical speed. v_{qds1}, v_{qds2}, v_{qdr1} and v_{qdr2} are stator and rotor q-d axis voltages. i_{qds1}, i_{qds2}, i_{qdr1} and i_{qdr2} are stator and rotor q-d axis currents. $\emptyset_{qds1}$, $\emptyset_{qds2}$, $\emptyset_{qdr1}$ and $\emptyset_{qdr2}$ are stator and rotor q-d axis flux and p=d/dt. L_{m1} and L_{m2} is the magnetizing inductance, and L_{r1}, L_{s1}, L_{s1} and L_{s2} are rotor and stator inductances.

B. MECHANICAL EQUATIONS

The total electromagnetic torque (C_e) is the sum of two components caused by the electromagnetic interaction between stator "1" and rotor and the interaction between the stator $\langle\langle 2\rangle\rangle$ and the rotor. Equation (11), gives this relation [29].

$$C_e = \frac{3}{2}p_1\mathrm{Im}\left[\underline{\phi}_{qds1}\ \underline{i}_{qds1}\right] + \frac{3}{2}p_2\mathrm{Im}\left[\underline{\phi}_{qds2}\ \underline{i}_{qds2}\right] \tag{11}$$

The fundamental dynamic equation of the dual stator machine can then express the DSM roto mechanical speed to the electromagnet torque and load, as it in equation (12). J and B_s are the inertia and friction factors, respectively.

$$\omega_m = \frac{C_e - C_l}{(J.s + B_s)} \tag{12}$$

IV. DIRECT TORQUE CONTROL (DTC) OF STATOR INDUCTION MOTOR

As expressed in the previous sections, the direct torque control loop is selected for controlling this machine. This technique appeared in the 80's and is developed by: I. Takahashi and Depenb [30]–[32]. It is a technique that allows direct and individual control of the motor torque by selecting the optimal switching modes of the inverters. First, the Electromagnetic torque and stator flux are calculated from the primary motor inputs, e.g., stator voltages and currents. Then, the selection of the optimal voltage vector is applied inside the inverter. Generally, the purpose of this control is to regulate the stator flux and electromagnetic torque without having measured the speed, flux, or torque, except those measurements of voltages and currents are used.

A. STATOR FLUX, ELECTROMAGNET TORQUE, AND SECTOR ESTIMATION MODEL

It is mandatory to express the used mathematical models for estimating the fluxes and electromagnet torque.

The expressions of the two fluxes into the two stators can be evaluated as it is in equations (13) to (15)

$$\begin{cases} \phi_{s1} = \sqrt{\phi_{s1\alpha}^2 + \phi_{s1\beta}^2} \\ \phi_{s2} = \sqrt{\phi_{s2\alpha}^2 + \phi_{s2\beta}^2} \end{cases} \tag{13}$$

where all the variables in equation (13) were given in (14) and (15).

$$\begin{cases} \phi_{s1\alpha} = \int_0^t (u_{s1\alpha} + R_{s1}i_{s1\alpha})\,dt \\ \phi_{s1\beta} = \int_0^t (u_{s1\beta} + R_{s1}i_{s1\beta})\,dt \end{cases} \tag{14}$$

And

$$\begin{cases} \phi_{s2\alpha} = \int_0^t (u_{s2\alpha} + R_{s2}i_{s2\alpha})\,dt \\ \phi_{s2\beta} = \int_0^t (u_{s2\beta} + R_{s2}i_{s2\beta})\,dt \end{cases} \tag{15}$$

where $\emptyset_{s1\alpha}$, $\emptyset_{s2\alpha}$, $\emptyset_{s1\beta}$ and $\emptyset_{s2\beta}$ represents the flux stators according to the axes (α, β). $u_{s1\alpha}$, $u_{s2\alpha}$, $u_{s1\beta}$ and $u_{s2\beta}$ represents the voltages stators according to the axes (α, β) and $i_{s1\alpha}$, $i_{s2\alpha}$, $i_{s1\beta}$ and $i_{s2\beta}$ represent the currents stators according to the axes (α, β).

So, the estimation of the angles of the first and second stators noted, respectively, θ_{s1} and θ_{s2} is calculated from equation (16).

$$\begin{cases} \theta_{s1} = arctg\dfrac{\phi_{s1\beta}}{\phi_{s1\alpha}} \\ \theta_{s2} = arctg\dfrac{\phi_{s2\beta}}{\phi_{s2\alpha}} \end{cases} \tag{16}$$

TABLE 1. Switching table for one stator.

Sector		S1	S2	S3	S4	S5	S6
$C_{flx}=1$	$C_{cpl}=1$	V2	V3	V4	V5	V6	V2
	$C_{cpl}=0$	V7	V0	V7	V0	V7	V0
	$C_{cpl}=-1$	V6	V1	V2	V3	V4	V5
$C_{flx}=0$	$C_{cpl}=1$	V3	V4	V5	V6	V1	V2
	$C_{cpl}=0$	V0	V7	V0	V7	V0	V7
	$C_{cpl}=-1$	V5	V6	V1	V2	V3	V4

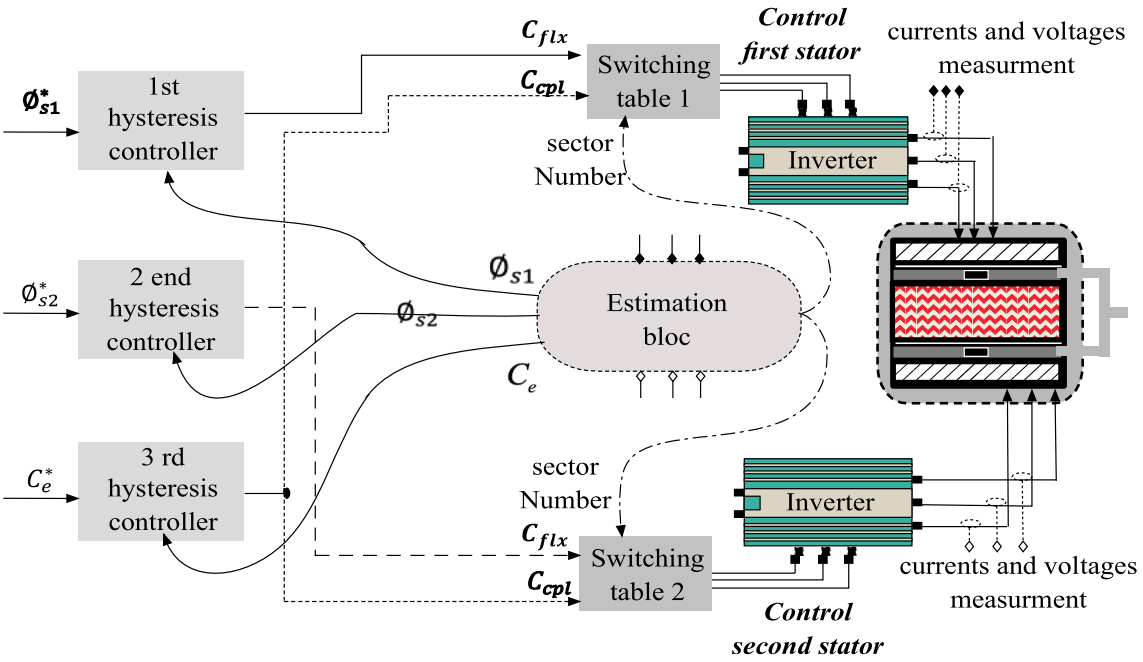

FIGURE 3. The scheme of the conventional DTC control.

TABLE 2. Fuzzy sets for each input variable.

Fuzzy sets	*Small (S)*		*Null (N)*		*Large (L)*	
Flux 1 error	<-1		-1<<1		1<	
Flux 2 error	<-0.5		-0.5<<0.5		0.5<	
Torque error	<-30		-30<<30		30<	
Fuzzy sets	***fourth***	***fifth***	***sixth***	***first***	***second***	***third***
Flux 1 angle	<-2 or 2<	-3<<-1	-2<<0	-1<<1	0<<2	1<<3
Flux 2 angle	<-2 or 2<	-3<<-1	-2<<0	-1<<1	0<<2	1<<3

On the other side, the estimation of the electromagnet torque can be evaluated as it is expressed in equation (17).

$$C_e = p\frac{L_m}{L_r}K\phi_{s1}\phi_r \sin\delta_{\phi 1} + p\frac{L_m}{L_r}K\phi_{s2}\phi_r \sin\delta_{\phi 2} \quad (17)$$

K represents the motor constant, $\delta_{\emptyset 1}$ and $\delta_{\emptyset 2}$ represent the angles between stator1, stator $\langle\langle 2\rangle\rangle$ and rotor flux vector, respectively.

B. THE CONVENTIONAL DTC ARCHITECTURE

The conventional architecture of this control loop is based on two hysteresis comparators, which compare the estimated values with the reference values for each flux and torque. Then the inverter states are selected, referring to switches tables. The measured amplitudes of the stator fluxes and electric torque are compared to their reference values. So, the outputs of the comparators with the number of sectors are located as it is in Table (1) [33], [34]. Table 1 shows the switching selection table for the stator flux vector in the first sector of the d-q plane [25]. The synoptic of the direct torque control loop for the dual stator machine can be shown in Fig. 3. Finally, the estimation block regroups all the equations (13) to (17) and estimates the necessary sector number accordingly to the angular positions.

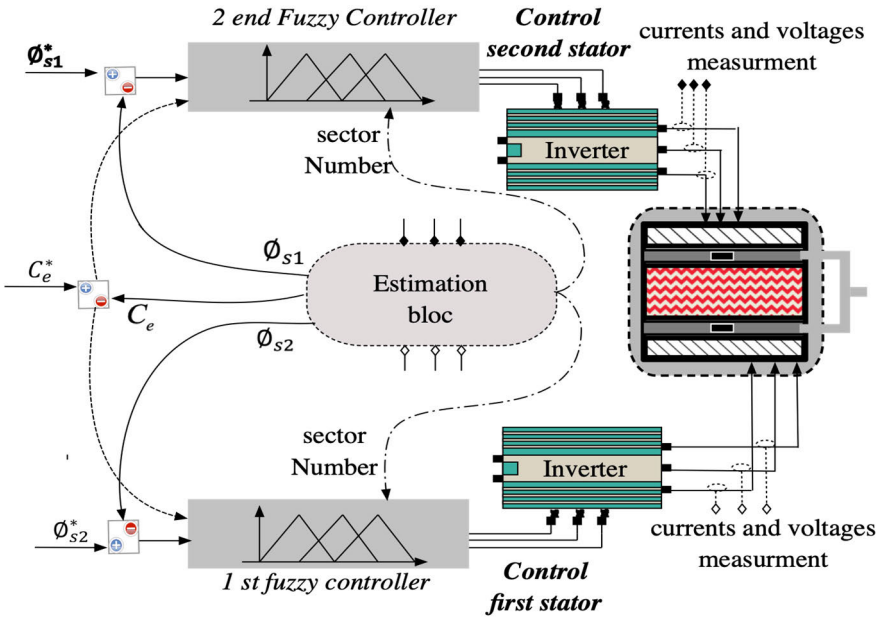

FIGURE 4. The scheme of the Fuzzy-DTC control loop.

TABLE 3. The 54 Rules description for feeding the first stator.

Rules	*Input vector*			*Output (S1, S2, S3)*
	Flux 1 error	*Torque error*	*Flux 1 angel*	
R1	Small	Small	first	000
R2	Small	Small	second	010
R3	Small	Small	third	011
R4	Small	Small	fourth	110
R5*	Small	Small	fifth	001
R6	Small	Small	sixth	101
		R7⇢ *R*48		
R49	Large	Large	first	101
R50	Large	Large	second	010
R51	Large	Large	third	111
R52	Large	Large	fourth	011
R53	Large	Large	fifth	011
R54	Large	Large	sixth	100
R5: is explained in Fig. 5)*				

In a voltage source inverter, eight switching positions can be chosen. The selection of a voltage vector is made to keep the torque and stator flux within the limits of two hysteresis. It is important to indicate that the hysteresis comparators for flux control are with two levels, and for electromagnetic torque control, it is the other with three levels.

C. THE FUZZY DTC ARCHITECTURE

For improving the performances of the conventional direct torque control loop the fuzzy logic controller was designed and implemented inside the DTC architecture. It is for having better performance when controlling the dual stator machine. The problems of torque and flux ripples and the bad performance of the motor speed when this machine is in motor

TABLE 4. The 54 rules description for feeding the second stator.

Rules	Input vector			Output (S1, S2, S3)
	Flux 2 error	Torque error	Flux 2 angel	
R1	Small	Small	first	010
R2	Small	Small	second	011
R3	Small	Small	third	001
R4	Small	Small	fourth	110
R5	Small	Small	fifth	100
R6	Small	Small	sixth	001
		R7⋯→ *R*48		
R49	Large	Large	first	101
R50	Large	Large	second	111
R51	Large	Large	third	110
R52	Large	Large	fourth	100
R53	Large	Large	fifth	000
R54	Large	Large	sixth	011

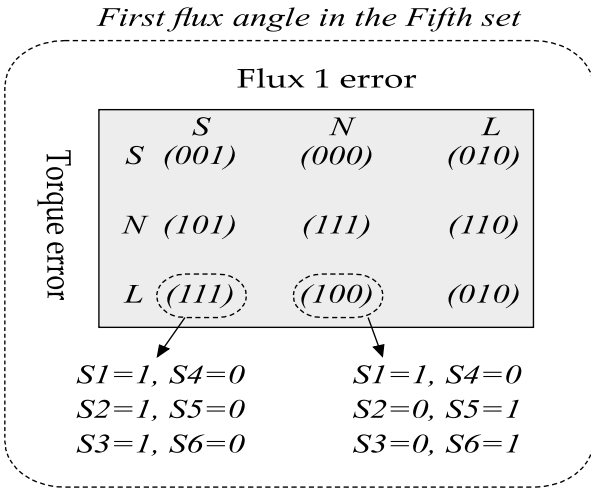

FIGURE 5. Combination of the switches for feeding the first stator if the fifth angular position is selected.

mode have obliged to improve this control solution. So, basing on the benefits of the fuzzy logic controller, the DTC is designed in another version using the fuzzy controllers face the hysteresis solution. The principle of the updated DTC loop becomes based on two fuzzy controllers, which use each one the error, between the real and the reference flux and electromagnet torque and use the estimated angular position of each stator face the rotor. At the same time, each of these fuzzy controllers will be directly responsible for the switching table outputs. This architecture is designed in Fig. 4.

1) THE FUZZIFICATION STEP

The fuzzy controller will directly manage the switching table loop, the flux error position for the first and the second stator, and the electromagnet torque error will be fuzzified. Then, the membership function for each of these variables will be fixed. Three membership functions for each of these variables is selected, and the triangular function type is chosen. However, six membership functions are selected for the fuzzy controller's third input parameter concerning the first and second flux positions. Table (2) summarizes all of these membership functions.

2) THE DEFUZZIFICATION STEP

The output variables are divided into three binary outputs according to the three switches of each of the two used inverters. So, two fuzzy sets represent the statue of each switcher.

3) THE RULES

The number of fuzzy rules designed for this improved DTC architecture regroups 54 rules, and the Mamdani method is the used inference method. So, Fig. 5 shows the case of all the rules if the fifth angular position is selected. Table (3) regroups all the rules for the first stator feeding, and Table (4) shows the designed rules for the second stator part. It is essential to indicate that the two tables will not show the same rules as two different stators will be controlled. For example, suppose the two stators have the same specification. Then, it is possible to make the same rules for the two controllers, and even it is possible to have only one fuzzy controller,

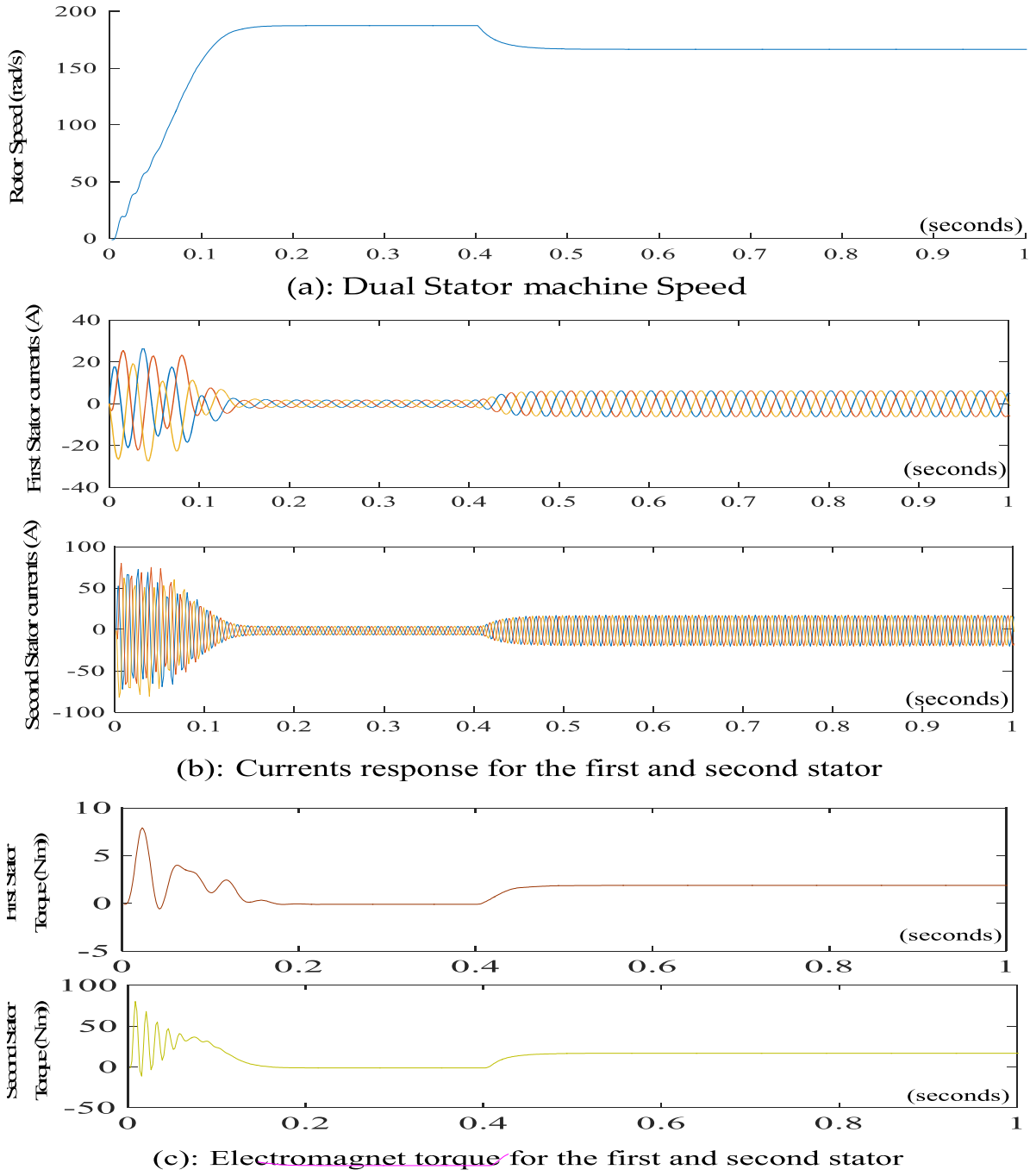

FIGURE 6. Speed, currents, and torques evolution for the Dual stator machine.

which can control the two stators parallelly. But in this case, no independence exists between the two stators.

V. SIMULATIONS RESULTS

The presented DTC control topology simulation tests for the dual stator machine monitoring have been carried out. Both stator windings were designed using the parameters of a 3-hp induction machine. The used dual stator motor specification and the inverter's specifications are summarized in Table (5). The simulation test will compare the performances of the conventional DTC control loop and the Fuzzy DTC control loop. It supervises the evolution of fluxes, electromagnet, and motor speed if the machine is used under the motor mode. So, initially, the reference motor speed is given for touching 150 rad/s as a ramp form, and at the instance of 0.4 seconds, a load torque will be applied. Then, the simulation test is made under a total time equal to 2 seconds. For the conventional DTC control loop, the used hysteresis bounds are

TABLE 5. Dual stator machine specification.

Parameters	*First stator*	*Second stator*
Power	2.2 kw	
Voltage	47 V	145 V
Stator inductance	0,14 H	0.04 H
Rotor inductance	0,04 H	
frequency	30 Hz	60 Hz
Poles number	2	6
Nominal Flux	1Wb	0.5Wb
Stator resistance	0,435	0,435
Rotor resistance	0,816	
Inertia factor	0.089 kg.m^2	
Nominal Speed	188.5 rad/s	
Friction coefficient	0 N.m.s/rad	
Inverter specifications		
DC voltage	600 V	
Switching frequency	20 kHz	

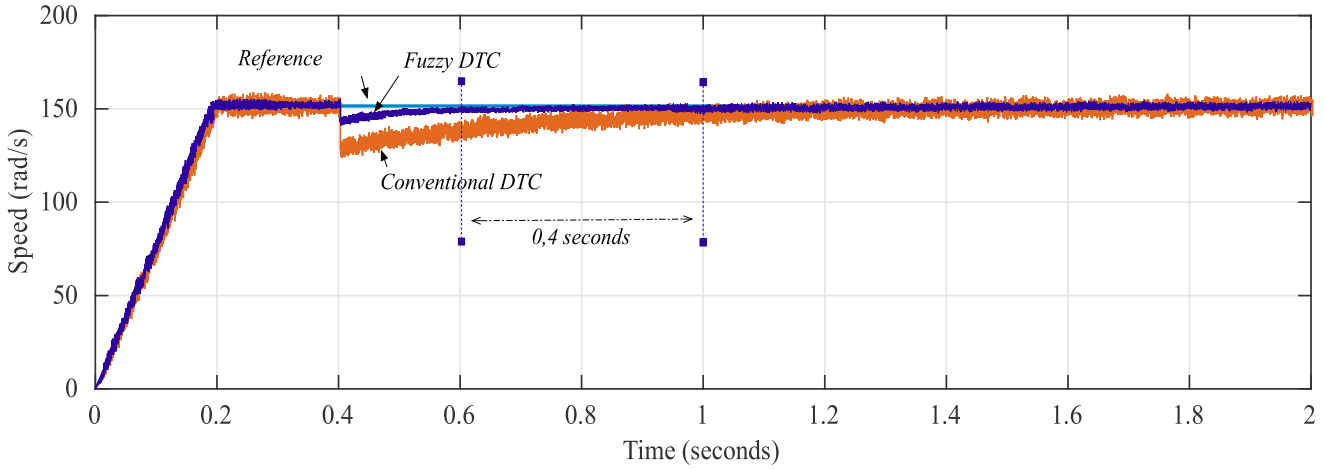

FIGURE 7. Speed, evolution with the conventional and fuzzy DTC architectures.

$\mp 0.005Wb$ and $\mp 0.5N.m$ for the fluxes and electromagnet torque respectively.

A. FIRST SIMULATION TEST: UNCONTROLLABLE DSM

Initially, it is mandatory to verify if the DTC architecture and the used motor equations are correctly inserted and used if all the simulation blocs are running correctly. So, an initial step tries to simulate the comportment of the dual stator machine without applying any torque load. So, for a no-load operation "Cr=0", from 0 to 0,4 seconds and for a nominal speed value equal to (188.5 rad/s), the depicted results in Fig. 6, validate that the inserted model is validated. The high performance of the built machine model is verified and validated by the given results, which show that there is total independence between the electromagnet torque and currents. Also, the current figure shows and validates that the two stators are controlled with two different frequencies. It is also apparent in the electromagnet torques. From 0,4 seconds, a load torque is applied "Cr=20 N. m", and then it is clear that if no control lop is operated, the motor speed will decrease, and the currents will increase. The corresponding electromagnet torques can be visualized in Fig. 6.c. The two stators collaborate to feed the motor with the necessary power.

B. SECOND SIMULATION TEST: A CONTROLLABLE DSM

As cited in the previous sections, the direct torque control loop will control this dual stator machine. It is by giving a reference speed ramp form as it is in Fig. 7. 150 rad/s is the nominal speed at the steady-state, and this is for 2 seconds as the total time of the simulation. At 0.4 seconds, a load torque is applied, and it is evident in Fig. 5 that the control loop compensates for the shutdown of the motor speed. However, Fig. 7 shows that the ripples are more important than the fuzzy-DTC loop with the conventional DTC form and with the best hysteresis configuration. Also, the response time with the fuzzy-DTC is better than the conventional DTC form.

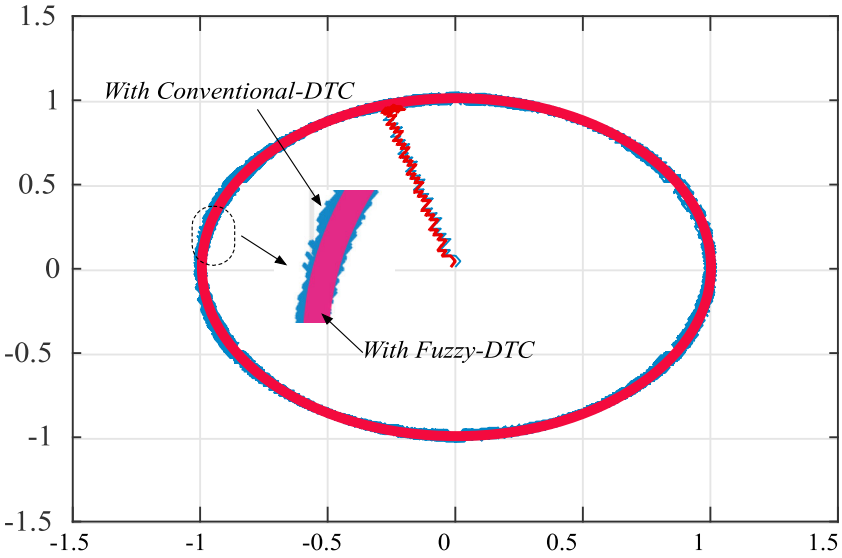

FIGURE 8. First Flux evolution with the conventional and fuzzy DTC architectures in the 2D-plan $((\alpha - \beta))$.

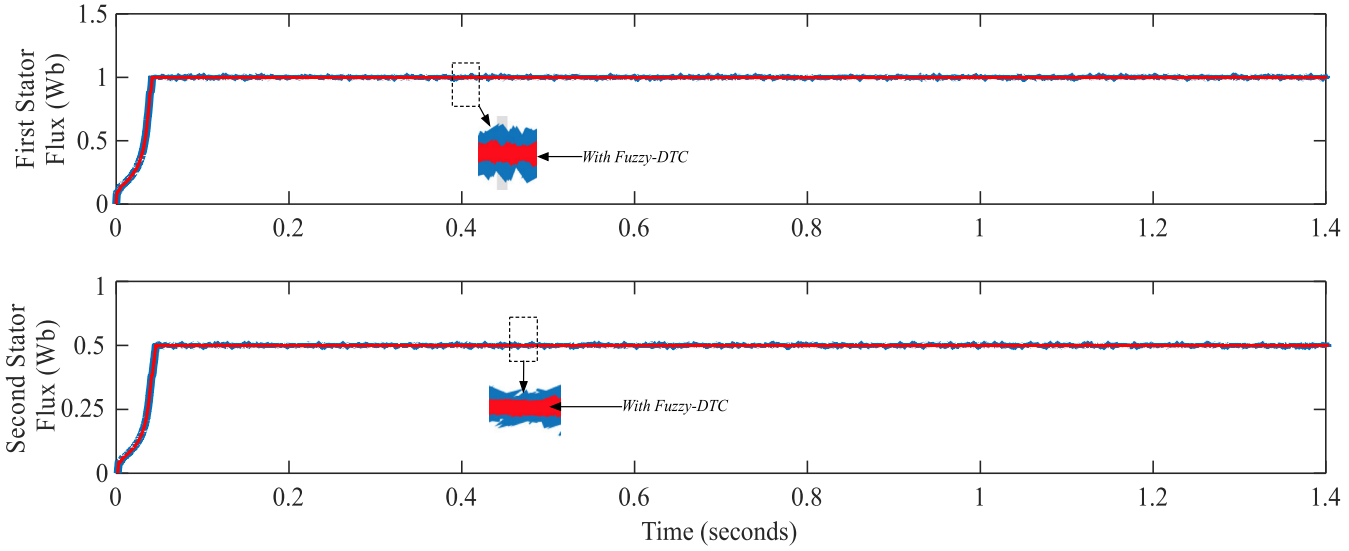

FIGURE 9. First stator Flux $\emptyset_{s1}$, and Second stator Flux $\emptyset_{s2}$, evolution with the conventional and fuzzy DTC architectures.

Therefore, there is a gain of 0, 4 seconds for making the speed response stable.

On the other side, the evolution of the electromagnetic torque Ce, of this machine if using the conventional DTC or the fuzzy-DTC architecture is presented in Fig. 10. Also, this figure, shows that the torque ripple was minimized, and better electromagnet performances appear. Also, in the 2D plane, it is possible to supervise the evolution of the first and second stator's flux, as shown in Fig. 8. Finally, the good performances of the Fuzzy-DTC are clearly shown in Fig. 9 and Fig. 8. All fluxes' ripples were eliminated, and the fluxes do not contain a high ripple factor.

Also, the fuzzy DTC version has a good performance on the stators currents, as it is in Fig. 11. In Fig. 11, only one phase current is shown, and it is clear that many fluctuations and ripples on the current were eliminated. Also, Fig. 12, shows a good performance for the second stator currents and it looks that with the Fuzzy-DTC topology, many fluctuations on the currents were eliminated. However, it is also clear that the current curve still presents some ripples, and this is because the second fuzzy controller set rules that need some updates.

The independence of the two stators' currents can be depicted in Fig.11 and Fig. 12, which show the phase A currents form for each stator. When a load torque was applied at 0.4 seconds, it is clear that the two currents of the same phase don't react in the same manner. Only the current of phase A of the second stator reacts. No reaction of the current

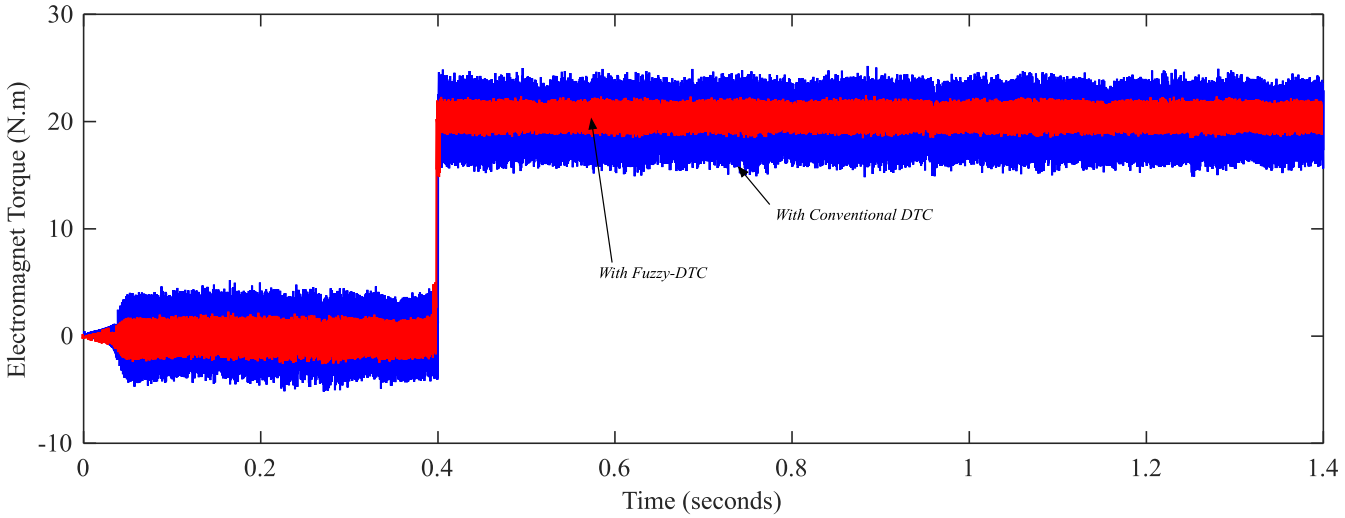

FIGURE 10. Response of Total electromagnet torque, with the two DTC architectures.

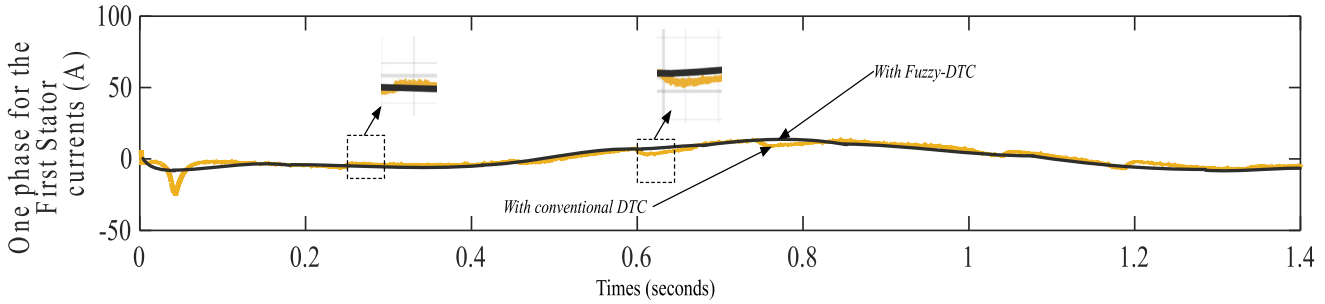

FIGURE 11. Response of one phase current for the first stator, with the two DTC architectures.

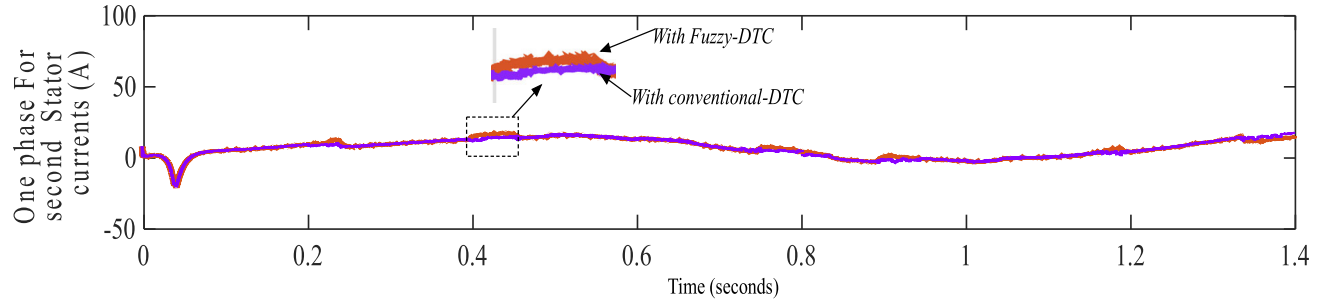

FIGURE 12. Response of one phase current for the second stator, with the two DTC architectures.

of the same phase for the other stator appears, which verifies the independence of the two controllers. The reaction will be on another phase as B or C, which proves that no dependence exists between the two stators. The used rules are verified and confirmed, which can prove that no similarity exists between the major rules for the two stators. Even the fluxes errors margins are not the same for the two stators. It can be validated by an example if concentrating on the fifth rule for the two stators. For the same conditions, the current of the phase A and C will be different. So, no similarity exists between the two stators. For more explanation for the role of the DTC fuzzy table, concentrating again at the instance 0.4 sec. At this point, the Flux error for the two stators is classified as small; however, for the torque error, the error value can be evaluated as 20 (N.m), and then the error torque can be classified as Null. Here, the selected rules are from the list of R7 to R13. It is for the two stator cases. These rules do have not the same relations on the switchers, and if concentrating on the A-phase, the given switch combination will be as it is in this vector [0 0 1 0 0 1] for the R7 to R13 of the first stator respectively and [1 1 0 0 1 1] for the R7 to R13 of the second stator, respectively. Which validates why

the second stator reaction is clearer? If changing these rules, all of the results will be changed too. If the combination of the first stator becomes on the second, then the current of the other stator will react. All of this is related to the selected rules.

At the same time, and the instance 0.23 seconds, the two currents show no dependence between the two controllers. It is important to indicate that this phenomenon is related to the fixed rules in Table (3) and (4).

VI. CONCLUSION AND PERSPECTIVES

This paper dealt with a direct torque control (DTC) scheme designed for controlling a dual stator machine. Initially, the motor system was studied and modeled, and all the corresponding equations were given. Then, based on the hysteresis controller, the conventional direct torque control design was presented and explained next. As this traditional technique has numerous problems, such as the torque and flux ripples and especially the lousy motor speed performances, a modified direct torque control based on an intelligent algorithm was designed. First, the fuzzy logic controller was used for improving this control topology method, and then the corresponding fuzzy controllers were designed. With this ameliorated control topology, the results show better performances and good behavior for the reference speed.

New performances mandatory test other amelioration solutions and increase the global rentability of this machine. So, working on twelve sectors seems to decrease the ripples in the fluxes and torques. Also, testing the usefulness of the optimization algorithms by an online adjusting the hysteresis control parameters can offer more good performances.

REFERENCES

[1] F. Creedy, "Some developments in multi-speed cascade induction motors," *J. Inst. Electr. Eng.*, vol. 59, no. 301, pp. 511–532, May 1921.

[2] F. Mehedi, R. Taleb, A. B. Djilali, and A. Yahdou, "SMC based DTC-SVM control of five-phase permanent magnet synchronous motor drive," *Indonesian J. Elect. Eng. Comput. Sci.*, vol. 20, no. 1, pp. 100–108, 2020.

[3] A. M. Lulhe and T. N. Date, "A technology review paper for drives used in electrical vehicle (EV) & hybrid electrical vehicles (HEV)," in *Proc. Int. Conf. Control, Instrum., Commun. Comput. Technol. (ICCICCT)*, Dec. 2015, pp. 632–636.

[4] K. Marouani, L. Baghli, D. Hadiouche, A. Kheloui, and A. Rezzoug, "A new PWM strategy based on a 24-sector vector space decomposition for a six-phase VSI-fed dual stator induction motor," *IEEE Trans. Ind. Electron.*, vol. 55, no. 5, pp. 1910–1920, May 2008.

[5] G. Wang, M. Yang, L. Niu, X. Gui, and D. Xu, "A static current error elimination algorithm for PMSM predictive current control," *Zhongguo Dianji Gongcheng Xuebao/Chin. Soc. Electr. Eng.*, vol. 35, no. 10, pp. 2544–2551, 2015.

[6] Y. Luo and Z. Ke, "Speed estimation rotor flux vector-controlled induction motor drive with motor resistance parameter identification," *Smart Sci.*, vol. 6, no. 4, pp. 363–373, 2018.

[7] A. Shukla and R. Sharma, "Modified DTC with adaptive compensator for low-speed region of induction motor in electric vehicle applications," *Smart Sci.*, vol. 8, no. 3, pp. 101–116, 2020.

[8] E. Levi, "Multiphase electric machines for variable-speed applications," *IEEE Trans. Ind. Electron.*, vol. 55, no. 5, pp. 1893–1909, May 2008.

[9] J. R. Vazquez and P. Salmeron, "Active power filter control using neural network technologies," *IEE Proc.-Electr. Power Appl.*, vol. 150, no. 2, pp. 139–145, Mar. 2003.

[10] E. Levi, R. Bojoi, F. Profumo, H. A. Toliyat, and S. Williamson, "Multiphase induction motor drives—A technology status review," *IET Electr. Power Appl.*, vol. 1, no. 4, pp. 489–516, 2007.

[11] T. Ahmed, H. Kada, and A. Ahmed, "New DTC strategy of multi-machines single-inverter systems for electric vehicle traction applications," *Int. J. Power Electron. Drive Syst.*, vol. 11, no. 2, pp. 641–650, 2020.

[12] N. Bianchi and M. Dai Pre, "Vector control schemes for series-connected six-phase two-motor drive systems," *IEE Proc.-Electr. Power Appl.*, vol. 150, pp. 139–145, 2003.

[13] A. R. Munoz and T. A. Lipo, "Dual stator winding induction machine drive," *IEEE Trans. Ind. Appl.*, vol. 36, no. 5, pp. 1369–1379, Sep. 2000.

[14] J. M. Guerrero and O. Ojo, "Total airgap flux minimization in dual stator winding induction machines," *IEEE Trans. Power Electron.*, vol. 24, no. 3, pp. 787–795, Mar. 2009.

[15] U. C. Dikshit and R. K. Tripathi, "Direct torque control for dual three-phase induction motor drives," in *Proc. Students Conf. Eng. Syst. (SCES)*, Mar. 2012, pp. 1–6.

[16] S. Basak and C. Chakraborty, "Dual stator winding induction machine: Problems, progress, and future scope," *IEEE Trans. Ind. Electron.*, vol. 62, no. 7, pp. 4641–4652, Jul. 2015.

[17] A. Flah, I. A. Khan, A. Agarwal, L. Sbita, and M. G. Simoes, "Field-oriented control strategy for double-stator single-rotor and double-rotor single-stator permanent magnet machine: Design and operation," *Comput. Electr. Eng.*, vol. 90, pp. 1–15, Mar. 2021.

[18] D. Casadei, F. Profumo, G. Serra, and A. Tani, "FOC and DTC: Two viable schemes for induction motors torque control," *IEEE Trans. Power Electron.*, vol. 17, no. 5, pp. 779–787, Sep. 2002.

[19] A. Jidin, K. A. Karim, K. Rahim, L. R. L. V. Raj, S. Ramahlingam, and T. Sutikno, "A review on constant switching frequency techniques for direct torque control of induction motor," *Indonesian J. Electr. Eng. Comput. Sci.*, vol. 7, pp. 364–372, 2017.

[20] *Introduction I.I. Commande Vectorielle de la MSAP Pour l'asservissement en Vitesse ou en Position*, pp. 15–26.

[21] K. Bouhoune, K. Yazid, and M. S. Boucherit, "ANN-based DTC scheme to improve the dynamic performance of an IM drive," in *Proc. 7th IET Int. Conf. Power Electron., Mach. Drives (PEMD)*, 2014, pp. 1–6.

[22] V. Naik N, S. P. Singh, and A. K. Panda, "An interval type-2 fuzzy-based DTC of IMD using hybrid duty ratio control," *IEEE Trans. Power Electron.*, vol. 35, no. 8, pp. 8443–8451, Aug. 2020.

[23] S. Radhwane and M. Abdelkader, "Direct vector control scheme for a dual stator induction machine (DSIM) using fuzzy logic controller," *J. Adv. Res. Sci. Technol.*, vol. 1, no. 1, pp. 28–38, 2014.

[24] F. Aymen, M. Alowaidi, M. Bajaj, N. K. Sharma, S. Mishra, and S. K. Sharma, "Electric vehicle model based on multiple recharge system and a particular traction motor conception," *IEEE Access*, vol. 9, pp. 49308–49324, 2021.

[25] C. Hwang, C. J. Hong, and C. Chang, "The development of direct-drive high-speed brushless permanent magnet motors for machine tools," *Smart Sci.*, vol. 5, no. 1, pp. 21–38, 2017.

[26] D. Hammoumi, C. El Bekkali, M. Karim, M. Taoussi, N. El Ouanjli, and B. Bossoufi, "Direct controls for wind turbine with PMSG used on the real wind profile of essaouira-Morocco City," *Indonesian J. Electr. Eng. Comput. Sci.*, vol. 16, pp. 1229–1239, 2019.

[27] S. R. C. Ahmad, R. N. F. K. R. Othman, M. N. Othman, N. A. M. Zuki, F. A. A. Shukor, S. Z. M. Isa, Z. Ibrahim, and C. A. Vaithilingam, "Modeling and analysis of double stator slotted rotor permanent magnet generator," *Energies*, vol. 10, pp. 1–16, Mar. 2017.

[28] P. Gao, Y. Gu, and X. Wang, "The design of a permanent magnet in-wheel motor with dual-stator and dual-field-excitation used in electric vehicles," *Energies*, vol. 11, no. 2, p. 424, Feb. 2018.

[29] M. Hasoun, A. El Afia, and M. Khafallah, "Field oriented control of dual three-phase PMSM based vector space decomposition for electric ship propulsion," in *Proc. Int. Conf. Comput. Sci. Renew. Energies (ICCSRE)*, Jul. 2019, pp. 1–6.

[30] I. Takahashi and Y. Ohmori, "High-performance direct torque control of an induction motor," *IEEE Trans. Ind. Appl.*, vol. 25, no. 2, pp. 257–264, Mar./Apr. 1989.

[31] Y. L. N. Rao and G. Ravindranath, "Intelligent controllers for direct self control-SVPWM using sample orientation phase voltages," in *Proc. Int. Conf. Inventive Comput. Technol. (ICICT)*, Feb. 2020, pp. 989–993.

[32] H. Benbouhenni, "Seven-level direct torque control of induction motor based on artificial neural networks with regulation speed using fuzzy PI controller," *Iranian J. Elect. Electron. Eng.*, vol. 14, no. 1, pp. 85–94, 2018.

[33] S. A. A. Tarusan, A. Jidin, M. L. M. Jamil, K. A. Karim, and T. Sutikno, "A review of direct torque control development in various multilevel inverter applications," *Int. J. Power Electron. Drive Syst.*, vol. 11, no. 3, pp. 1675–1688, 2020.
[34] N. Mohamed, T. Hamza, and G. Brahim, "Novel DTC induction machine drive improvement using controlled rectifier for DC voltage tuning," *Int. J. Power Electron. Drive Syst.*, vol. 10, no. 3, p. 1223, Sep. 2019.

FLAH AYMEN was born in Gabès, Tunisia, in 1983. He received the bachelor's and M.Tech. degrees in electrical engineering from the National Engineering School of Gabès (ENIG), Tunisia, in 2007 and 2009, respectively, and the Ph.D. degree from the Department of Electrical Engineering, ENIG, in 2012. He has academic experience of 11 years. In 2021, he becomes an Associate Professor. He is currently an Associate Professor with ENIG, University of Gabès. He has published over 40 research articles in international cited journals and conferences and book chapters. His research interests include regroups, electrical vehicle applications, renewable energies, and power management.

NAOUI MOHAMED was born in Nefta, Tunis, in 1991. He received the degree in electrical engineering from the University of Gabès, Tunisia, in 2015. He is currently pursuing the Ph.D. degree in electrical engineering with the Research Unit Proceeds, Energies, Environment and Electrical Systems, National Engineering School of Gabès. He has published over 20 research articles in reputed journals, international conferences, and book chapters. His research interests include electric vehicle, power systems, and renewable energy.

SAAD CHAYMA was born in Tozeur, Tunisia, in 1996. He received the bachelor's degree in electrical automation from the University of Gabes, Tunisia, in 2019. He is currently pursuing the master's degree in electrical engineering with the Research Unit Proceeds, Energies, Environment and Electrical Systems, National Engineering School of Gabès.

C. H. RAMI REDDY (Member, IEEE) received the B.Tech. degree in electrical and electronics engineering and the M.Tech. degree in electrical machines and drives from Jawaharlal Nehru Technological University, Kakinada, Andhra Pradesh, in 2011 and 2014, respectively, and the Ph.D. degree in electrical and electronics engineering from K. L. University, Andhra Pradesh, India, in December 2020. He is currently working as an Assistant Professor in electrical and electronics engineering with Malla Reddy Engineering College (Autonomous), Secunderabad, Telangana, India. His current research interests include integrated renewable energy systems, distributed generation, FACTS devices, and power converters and their applications to energy systems. He is an editorial board member, a Reviewer of various *Web of Science* and *Scopus Indexed Journals*, and the Editor-In-Chief of *International Transactions on Electrical Engineering and Computer Science*, a quarterly publishing open access journal.

MOSLEH M. ALHARTHI was born in Taif, Saudi Arabia, in 1966. He received the B.Sc. and M.S. degrees in electronics technology and engineering from Indiana State University, Terre Haute, IN, USA, in 1996 and 1997, respectively, and the Ph.D. degree in electrical engineering from Arkansas University, Fayetteville, AR, USA, in 2001. He was an Assistant Professor with Jeddah College of Technology, Jeddah, Saudi Arabia, from 2001 to 2009. He is currently working as a Professor with the Electrical Engineering Department, Taif University, Saudi Arabia. He also works as the Dean of the College of Engineering, Taif University. His research interests include control engineering, electronics, and signal processing.

SHERIF S. M. GHONEIM (Senior Member, IEEE) received the B.Sc. and M.Sc. degrees from the Faculty of Engineering at Shoubra, Zagazig University, Egypt, in 1994 and 2000, respectively, and the Ph.D. degree in electrical power and machines from the Faculty of Engineering, Cairo University, in 2008. Since 1996, he has been teaching with the Faculty of Industrial Education, Suez Canal University, Egypt. From 2005 to 2007, he was a Guest Researcher with the Institute of Energy Transport and Storage (ETS), University of Duisburg–Essen, Germany. He joined the Electrical Engineering Department, Faculty of Engineering, Taif University, as an Associate Professor. His research interests include grounding systems, dissolved gas analysis, breakdown in SF6 gas, and AI technique applications.